DEVELOPING FE MODELS IN ORDER TO ACCURATELY PREDICT MATERIAL BEHAVIOUR OF PLASTIC

MD TARIQUL ISLAM |Internship report| 30/08/2017

PREFACE

This report presents the research, Finite Element (FE) modelling and analysis of plastic material as a part of an internship. It is the final report which will explain how the modelling is came about.

This internship is part of the first year curriculum of the masters in Computational mechanics at UPC, Barcelona. The aim of this internship is to give the student an opportunity to apply the theory taught during courses and stimulate working in a corporate environment.

I am thankful to FEMTO Engineering for accepting me as an intern and giving me the opportunity to learn and develop skills necessary for future carrier. I would also like to take this opportunity to express my gratitude to my internship supervisor Richard, who helped and guided me throughout, without which this report would have not been possible. I am also grateful to Sander, Alexander, Arjan, Micah and Stijn for helping me in this entire time period.

ABSTRACT

The available material data needed to perform FE simulation to assess the material behavior of plastic components are often limited. When stress-strain curves are available, they are not always suitable to implement directly in the FE model. Working with incomplete or un-validated FE models limits the reliability of the FE model.

The goal of this project is to obtain validated FE models in order to accurately understand material behavior of plastic. FE software FEMAP with NX NASTRAN is being used to carry out the modelling and analysis.

Table of Contents

1. INTRODUCTION

FE modelling has become integral part of any design process related to material and structure. Simulation followed by verification and validation lead to a more efficient and reliable design. This report deals with material behavior in terms of stresses and deflection under different loading conditions. FEMAP with NX Nastran is used to develop the FE models and to carry out the analysis. It is followed by validation process, where the simulation results are compared with real experimental result.

At first, a literature study is performed to find the standard codes and input parameters available. Relevant FE model are proposed based upon the input parameters which is presented in section 2 and 3. The details of FE model of uniaxial tensile test specimen can be found in section 4. In section 5, description of FE model for flexure test specimen is given.

Once the FE models are made, validation comes into act. Section 6 describes the validation process, where several simulations are run and the results are compared with the actual data. And at last, the report ends with a conclusion.

2. TYPES OF FE MODELS

FE models are popular for its ability to predict the behavior of materials and structure quite accurately. It remains as a powerful tool in the field of cutting-edge technological advancement in design and analysis.

In this very project, the FE model should be configured to match both uniaxial tensile test and flexural test. Therefore, two types of FE models are being developed in order to correctly predict the material behavior of plastic. They are:

- FE model for uniaxial tensile test

- FE model for Flexure test (three-point bending test)

These FE models are developed by maintaining international standards, namely: ASTM and ISO. For the tensile test, two FE models are created, one complying with ASTM D638 standards and other complying with ISO 527. For the flexure test, FE model complying with ISO 178 is made.

3. INPUT PARAMETERS AVAILABLE

One of the indispensable part of FE modelling is the input data that need to be feed into the FE model in order to resemble its behavior as close as possible to the real test data. Unlike metals, input data for plastic materials are not readily available. After a literature study session, it can be seen that the following material data can be found for various types of plastics:

- Young's modulus
- Tensile stress at yield
- Tensile stress at break
- Tensile strain at yield
- Tensile strain at break
- Density
- Poisson's ratio
- Stress-strain curve

Based upon the input data above, the following different material non-linearity type can be defined for the FE model:

1) Type A = Linear Elastic
2) Type B = Bi-Linear
3) Type C = Non-Linear Elastic

1) **Linear Elastic**

Input required: Young's modulus, Poisson's ratio, Mass density

2) **Bi-Linear**

Input required: Young's modulus, Poisson's ratio, Mass density, Tensile stress and strain at yield, Tensile stress and strain at break

3) **Non-Linear Elastic**

Input required: Young's modulus, Poisson's ratio, Mass density, stress-strain function

4. FE MODEL FOR UNIAXIAL TENSILE TEST SPECIMEN

Tensile test needs to be conducted on materials in order to determine its suitability for particular engineering interest and helps to understand the behavior of materials under loading conditions. Fig 1 below shows the dimensions of the tensile test specimen that is used for the tensile testing.

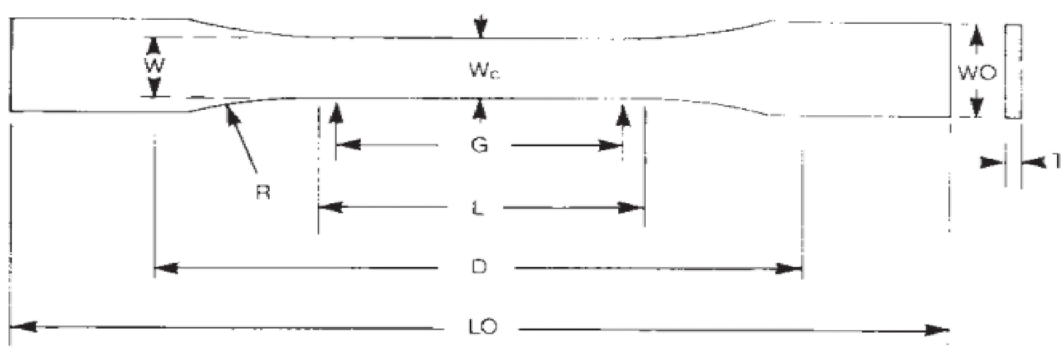

Fig 1: Tensile specimen dimension [1]

ASTM D 638	ISO 527
Length overall(LO) = 165 mm	Length overall (LO) = 165 mm
Distance between grips (D)= 115 mm	Distance between grips (D)= 115 mm
Distance between grips (L) = 57 mm	Distance between grips (L) = 59.5 mm
Gage length (G) = 50 mm	Gage length (G) = 50 mm
Width overall(WO)= 19 mm	Width overall(WO)= 19.5 mm
Width of narrow section (W) = 13 mm	Width of narrow section (W) = 10 mm
Radius of fillet(R) = 7 6mm	Radius of fillet(R) = 76 mm
Thickness = 7 mm	Thickness = 1 mm

Following the specimen dimensions illustrated in the previous page and using the FE software FEMAP with NX Nastran, two FE models for uniaxial tensile test has been developed. In fig 2 below is the tensile test FE model complying with ASTM D638 standard and in fig 3 is the tensile test FE model complying with ISO 527 standard.

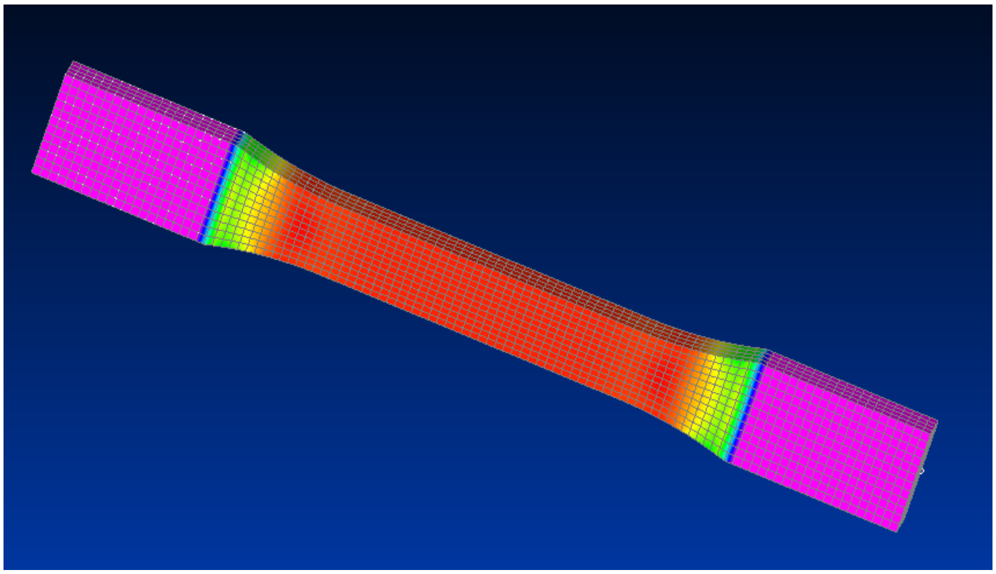

Fig 2: Tensile test FE model according to ASTM D638

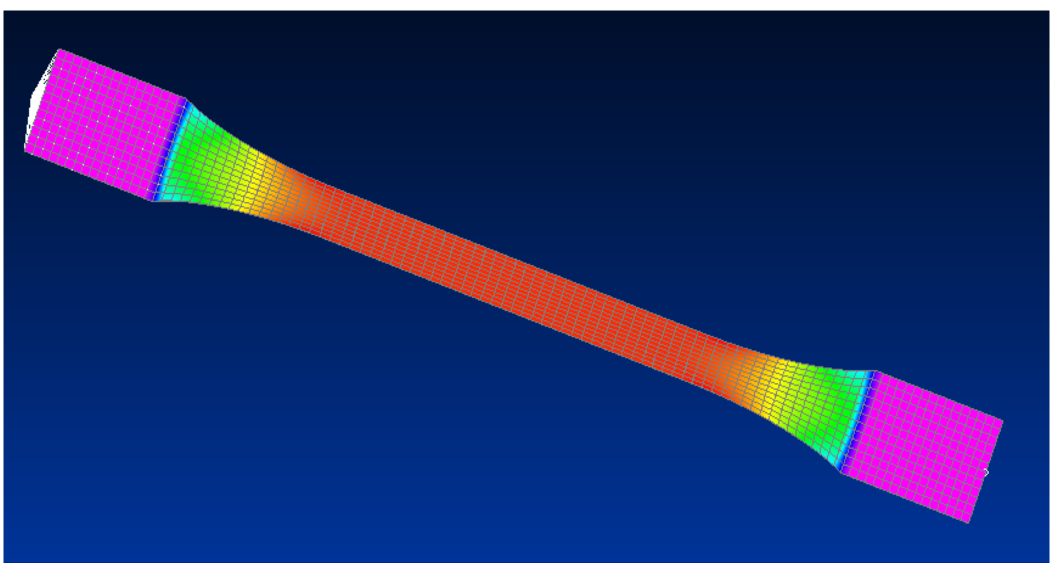

Fig 3: Tensile test FE model according to ISO 527

BI-LINEAR MODEL

Once the FE model for tensile test is developed, different non-linearity can be defined based upon the material data available. Lexan SLX-2432T plastic material is chosen for the investigation of its behavior. Its input parameters are sufficient to define bi-linear type nonlinearity. The input parameters based upon ASTM D638 and ISO 527 are:

Input Parameter for Lexan SLX -2432T		
	ASTM D638	ISO 527
Young's modulus	2550 MPa	2550 MPa
Tensile stress at yield	67 MPa	65 MPa
Tensile stress at break	72 MPa	69 MPa
Tensile strain at yield	6 %	6 %
Tensile strain at break	110 %	110 %
density	1.2 g/cm^3	1.2 cm^3
Poisson's ratio	0.35	0.35

Table 1: input parameters [2]

For the bi-linear model, plasticity modulus is required in addition to the young's modulus. Plasticity modulus can be calculated (from the given data above) by:

Plasticity modulus = $\frac{\text{stress at break} - \text{stress at yield}}{\text{strain at break} - \text{strain at yield}} = \frac{72-67}{1.1-0.06}$

= 4.807 MPa (ASTM D638)

= $\frac{69-65}{1.1-0.06}$

= 3.846 MPa (ISO 527)

Using all these input data, a bi-linear FE model has been developed. The simulation is run using the basic non-linear solver with an initial forced displacement of 15mm (30% of gauge length) applied on the specimen.

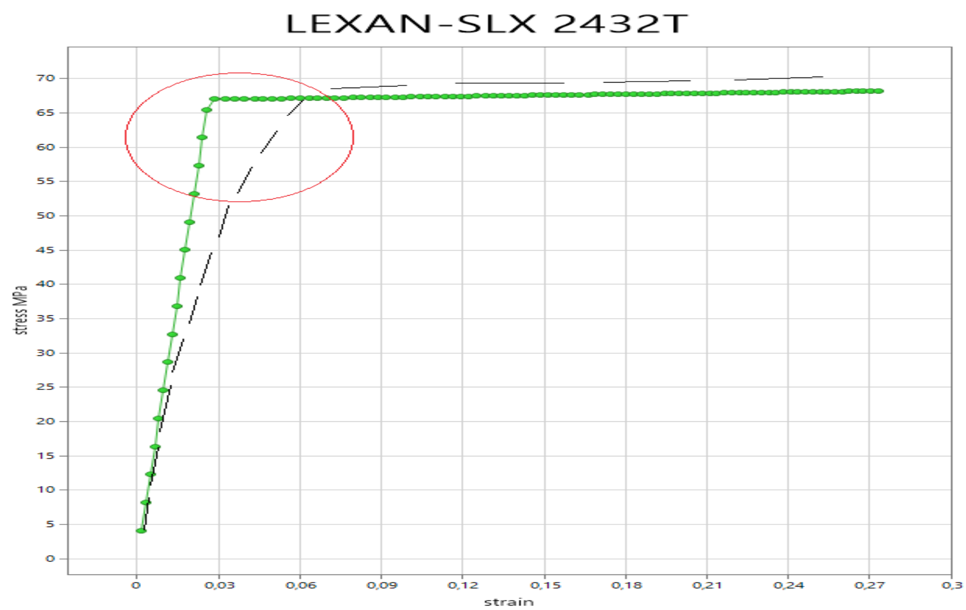

Fig 4: stress-strain graph of bi-linear model of Lexan-SLX 2432T (ASTM D638)

Fig 5: stress-strain graph of bi-linear model of Lexan-SLX 2432T (ISO 527)

In fig 4 and fig 5, the green lines represent the graph from the bi-linear model while the dotted black line is the probable graph for the real behavior of the material. In bi-linear model, both elastic and plastic part are modelled as linear. Linearity is based upon the young's modulus and plasticity modulus that is given as input. For plastic materials, non-linearity arises in both elastic and plastic part. This is the reason for the difference in results between simulation and real behavior.

The model works pretty well in predicting the real behavior of the material except in the region mentioned in red circle. Here the model overestimates the strength of the material while in real life the material already started to lose its strength.

For observing the behavior of the tensile test specimen under loading condition, the node experiencing the maximum stress within the FE model is considered. It might be often interesting to see how other nodes at different part of the tensile test specimen behaves. In order to know that, two nodes within the gauge length can be chosen, and their corresponding elongation with respect to forced displacement of the specimen can be observed.

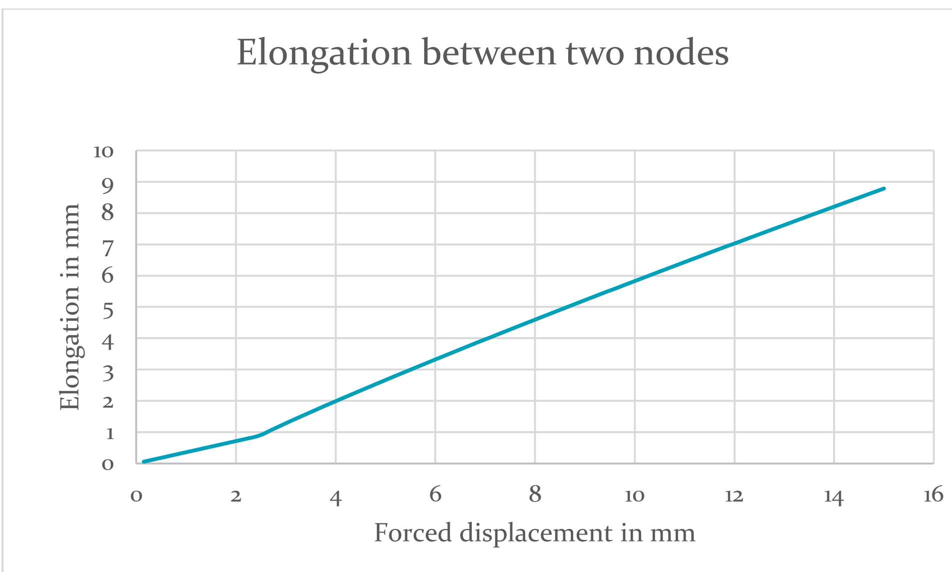

Fig 6: Elongation between two nodes.

Fig 6 shows how the distance between the nodes increases as the forced displacement on the specimen increases. From the above graph, the strains and corresponding stresses can be calculated. This gives more freedom in terms of choice of area within the FE model that can be chosen for observation.

It is also interesting to find out the results of simulation when different solvers are used. Apart from basic non-linear solver, advance non-linear solver can also be implemented.

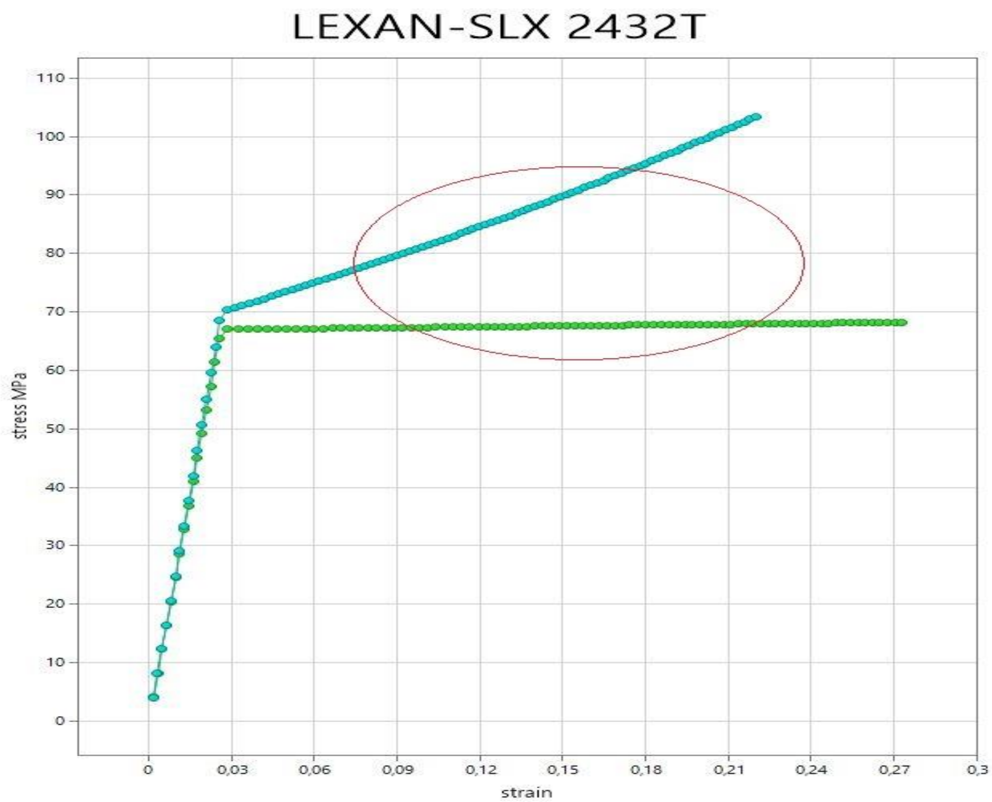

Fig 7: stress-strain graph of bi-linear model of Lexan-SLX 2432T (ASTM D638)

In fig 7, the blue line represent the graph from the advance nonlinear solver while the green line represent the graph from the basic nonlinear solver.

It is clearly seen that the graph retrieved using advance nonlinear solver not only overestimates the strength of the material in the elastic region but also in the plastic region (red circle). This made the solution unrealistic in terms of predicting the material behavior correctly. Therefore, advance nonlinear solver is not used for the analysis.

5. FE MODEL FOR FLEXURE TEST SPECIMEN

When a material is under loading, maximum of the time it is in the form of three point bending. If the young's modulus is same as the flexure modulus (e.g. for metals, steel etc.), then it is perfectly alright to use the young's modulus to determine the behavior of the material. But for plastic, it is not always the case that the young's modulus is same as flexure modulus. In this case, knowing the right flexure modulus is key in predicting the behavior of the material when subjected to bending.

Also when a specimen is under flexural loading, all three fundamental stresses are present: tensile, compressive and shear and so the flexure properties of a specimen are the result of the combined effect of all three stresses.

Fig 8 below shows the dimensions of the flexure test specimen that is used for developing FE model for flexure testing.

The difference in dimensions for ASTM and ISO flexure test specimen are negligible. Therefore only one FE model is developed, which is according to ISO 178 standard.

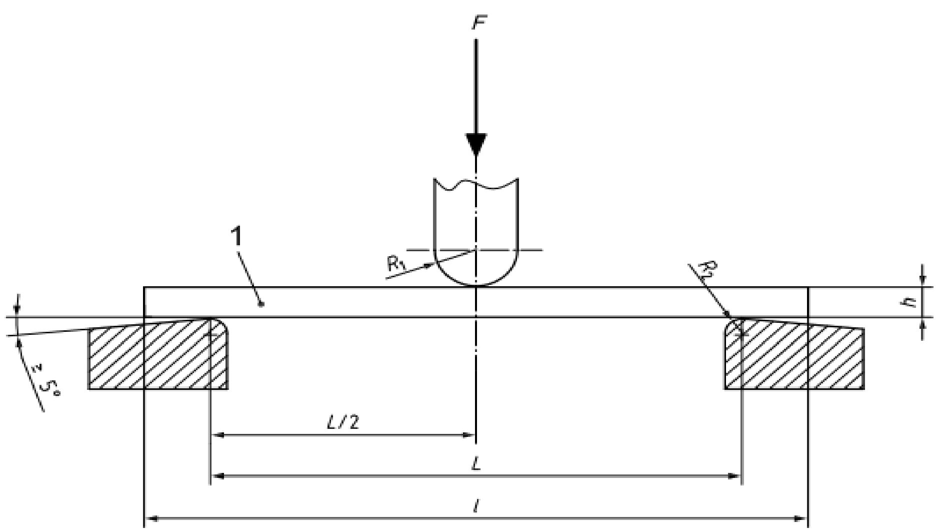

. Fig 8: Flexure specimen dimensions [3]

<u>ISO 178</u>

- Length overall (l) = 80 mm
- Length of span between support(L) = 64 mm
- Width = 10 mm
- Thickness (h) = 4 mm
- Radius of loading nose (R1) = 5 mm
- Radius of supports (R2) = 5 mm

A rectangular specimen, loading nose and loading support of aforementioned dimension are used for developing the FE Model. Fig 9 shows the FE model for Flexure testing:

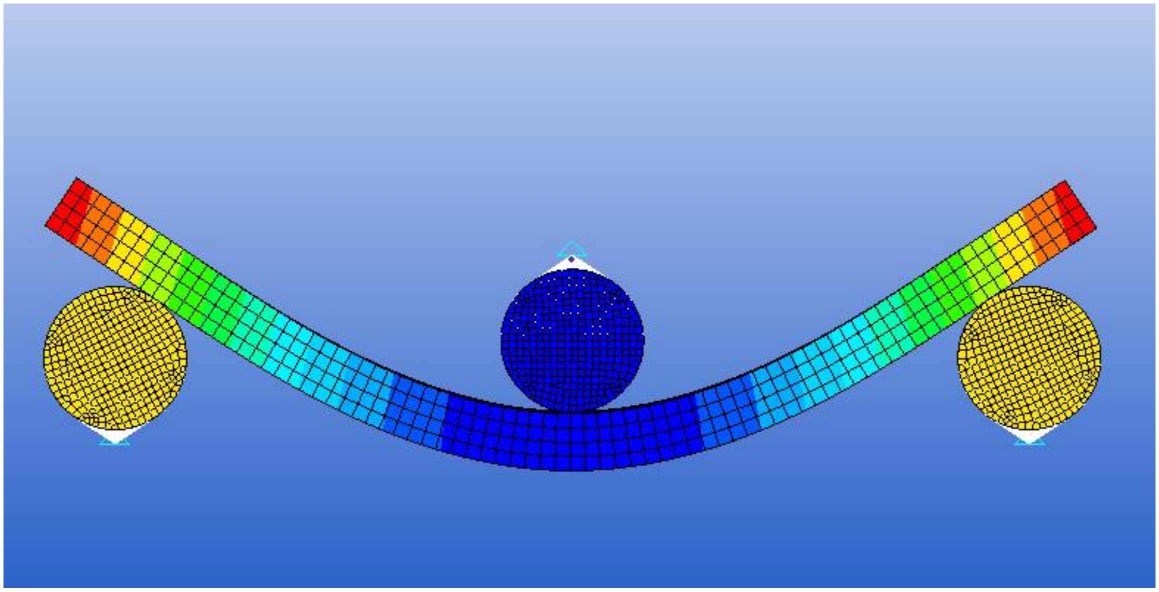

Fig 9: FE model for flexure test

A forced displacement is introduced to the specimen at mid-span using the cylindrical loading nose. This value needs to be calculated according to standard codes. According to ISO and ASTM, the test should be terminated when the maximum strain in the outer surface of the test specimen has reached 5% (0.05 mm/mm). The deflection at which this strain will occur is calculated using the following formula:

$$D = \frac{rL^2}{6d} \quad [4]$$

D = Mid-span deflection (mm)

r = strain (mm/mm) = 0.05

L = support span (mm) = 64 mm

D = thickness (mm) = 4mm

Plugging the values in the above equation, the deflection is calculated, which is found to be 12.8 mm. This deflection is introduced to the specimen in the FE model through the loading nose at mid span. Due to the contact properties being used in the model, simulation is run using advance non-linear solver.

Mid-section of the outer surface of the specimen is chosen to observe the variation of deflection compare to the variation of force in the loading nose. This is because, it is in this region where the specimen experience the maximum deflection. Once the analysis is complete, a load vs deflection graph is plotted.

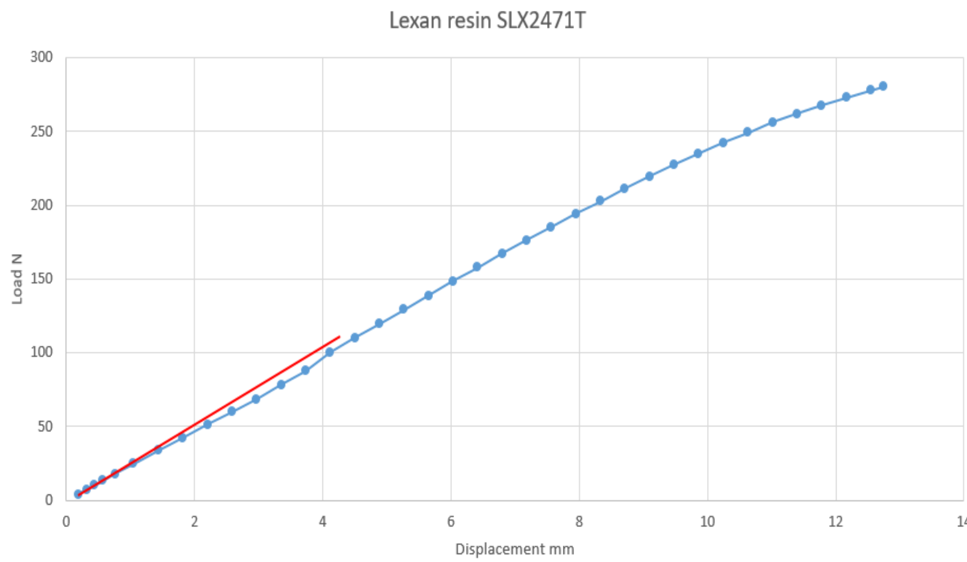

Fig 10: Load-displacement graph for SLX2471T.

In fig 10, the blue line represents variation of load along with the forced displacement on the specimen. The red line is the slope of the tangent to the steepest initial straight-line portion of the load-deflection curve (N/mm).

Finally, the flexure modulus is calculated using the following formula,

$$E_f = \frac{L^3 m}{4bd^3} \quad [4]$$

E_f = flexure modulus, d = thickness = 4mm

L = support span = 10mm, b = width = 10 mm

M = slope of the steepest initial straight line (N/mm)

6. SIMULATION AND VALIDATION

Validation is of paramount importance for any FE model being developed. It gives the indication that the model is working as it should. Invalidated FE model often leads to unrealistic results.

For the validation of the tensile and flexure model, real test data of plastic Ultem HU 1004 are available. The stress strain data from the real tensile test are given in fig 11 and fig 12:

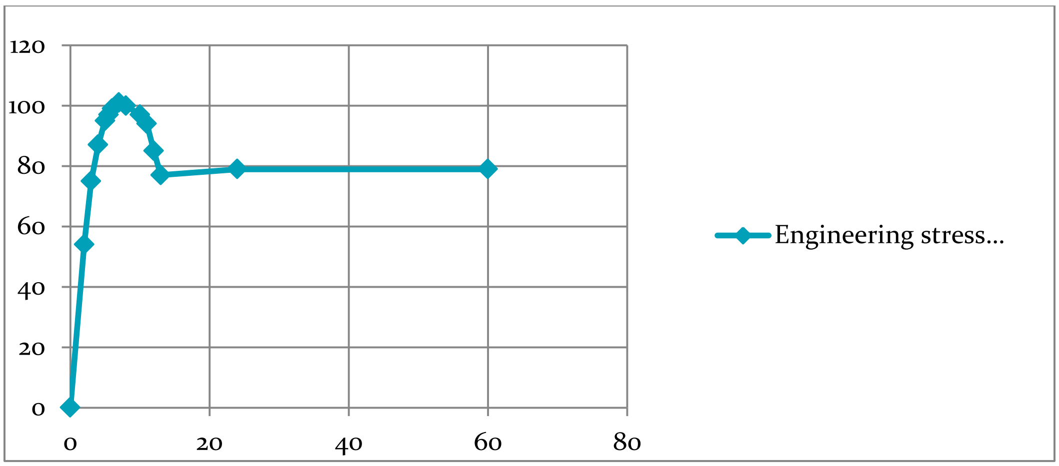

Fig 11: stress –strain (engineering) data

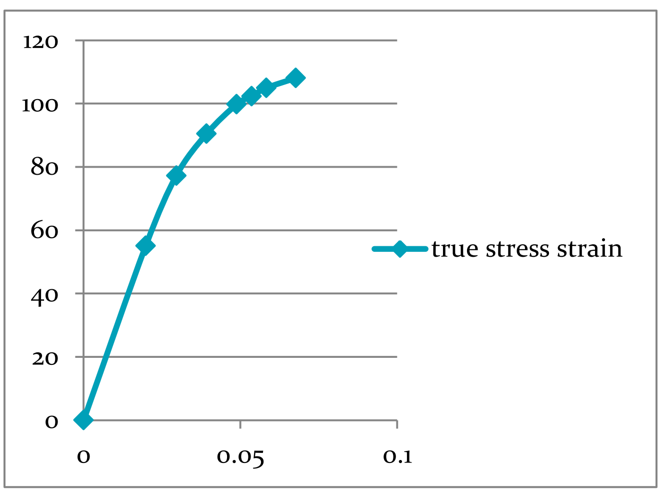

Fig 12: stress –strain (true) data

From the data sheet of Ultem HU1004, the input parameters are collected and are as follows:

Young's modulus: 2900 MPa

Poisson's ratio: 0.36

Mass density: 1.28 g/cm^3

Based upon the available information, a non-linear elastic model is made for the tensile specimen. The stress-strain curve along with the other input parameters are fed into the FE model and the behavior is observed. The simulation is run using the basic non- linear solver.

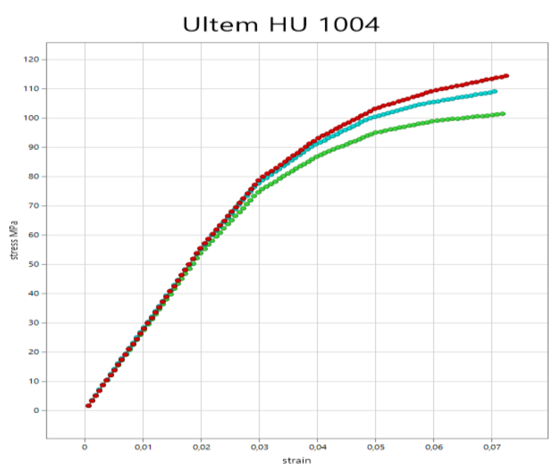

Fig 13: stress-strain graph of ASTM D638

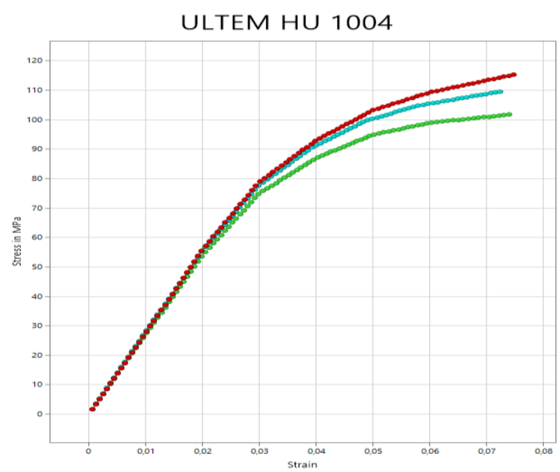

Fig 14: stress-strain graph of ISO 527

The green lines in the above graphs (fig 13 and fig 14) represent the engineering stress vs strain curve while the blue line represent true stress vs strain curve. The red curve is retrieved when advance non-linear solver is used. Technically, advance non-linear solver should give true stress-strain curve. But it can be seen it's not exactly same as the blue graph but an offset of 4.9%. This is because, when calculating true stress or strain (e.g. for steel), it is assumed that the volume remains constant until necking (AL $=A_0 L_0$), which might not be the case for plastic materials.

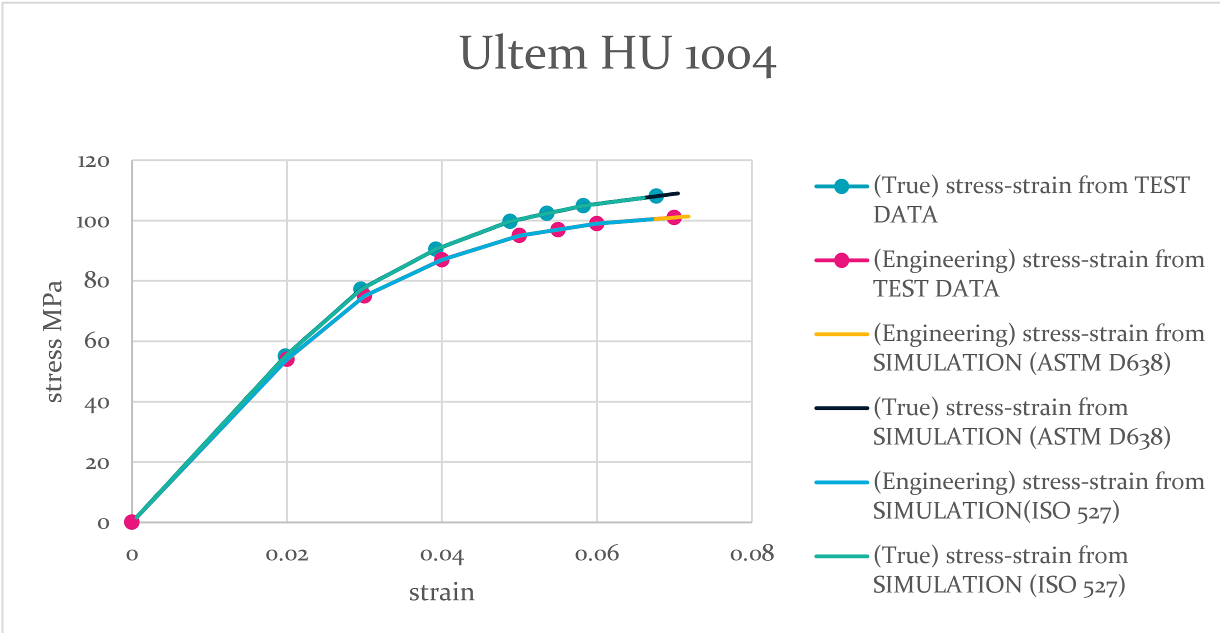

Fig 15: Combined stress-strain graph from the test data and simulation

When graphs from both simulation and real test data are plotted on top of each other (Fig 15), they match exactly.

For the flexure test FE model, the specimen is given a deflection of 12.8mm (as calculated earlier in this report). To account for the non-linearity, the stress-strain function is incorporated into the FE model. For the simulation, advance non-linear solver is used. Once the simulation is run and analysis is complete, load vs deflection graph is plotted which can be seen in fig 16.

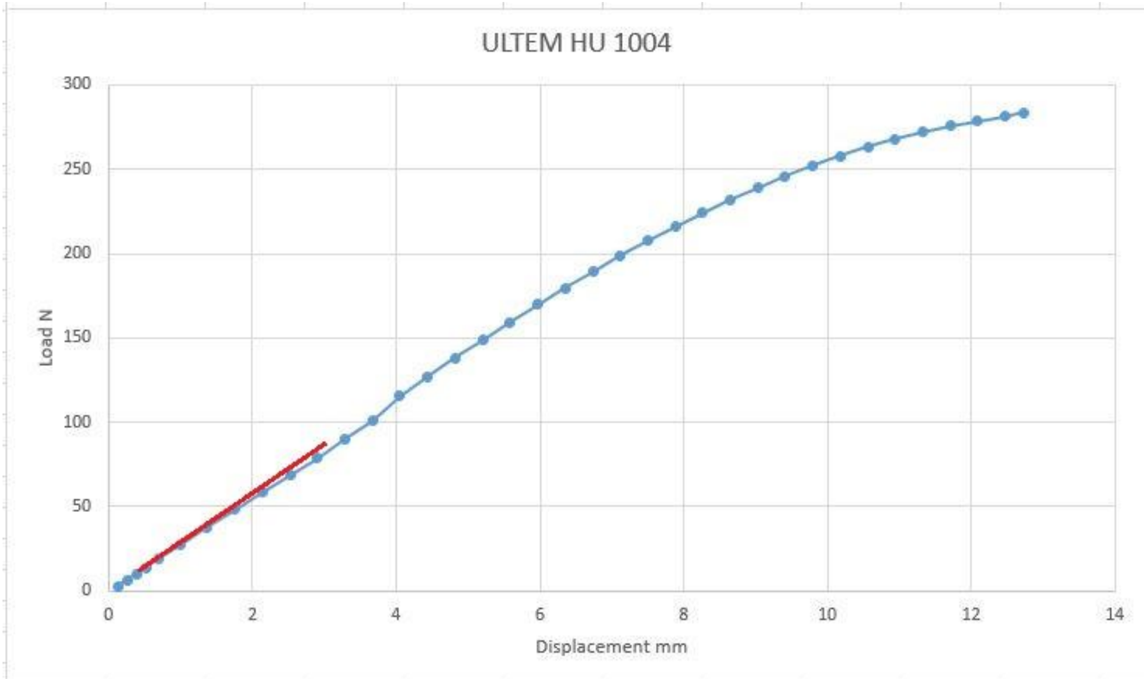

Fig 16: load-displacement graph for Ultem HU 1004

From the above graph, the slope of the steepest initial straight-line portion is calculated and found to be 27.35 N/mm. Plugging this value along with other parameters into the below equation, the flexure modulus is determined.

$$E_f = \frac{L^3 m}{4bd^3} \quad [4]$$

E_f = flexure modulus, d = thickness = 4mm

L = support span = 10mm, b = width = 10 mm

M = slope of the steepest initial straight line (N/mm) =27.35

The flexure modulus is found to be 2792 MPa, which is very close to the value 2800 from the test data.

BITE TEST SIMULATION

Once the specimen FE models are configured to match both uniaxial tensile test and flexure test, it needs to be implemented in existing FE models and validated with available experimental data.

A structure made up of plastic (Ultem HU 1004) material is modelled and subjected to a force from the bite of human teeth. In real life, the structure is made from two separate parts glued together to form a single structure. For the FE analysis, both the parts will be analyzed separately. In fig 17, the bottom half of the structure can be seen:

Bottom part

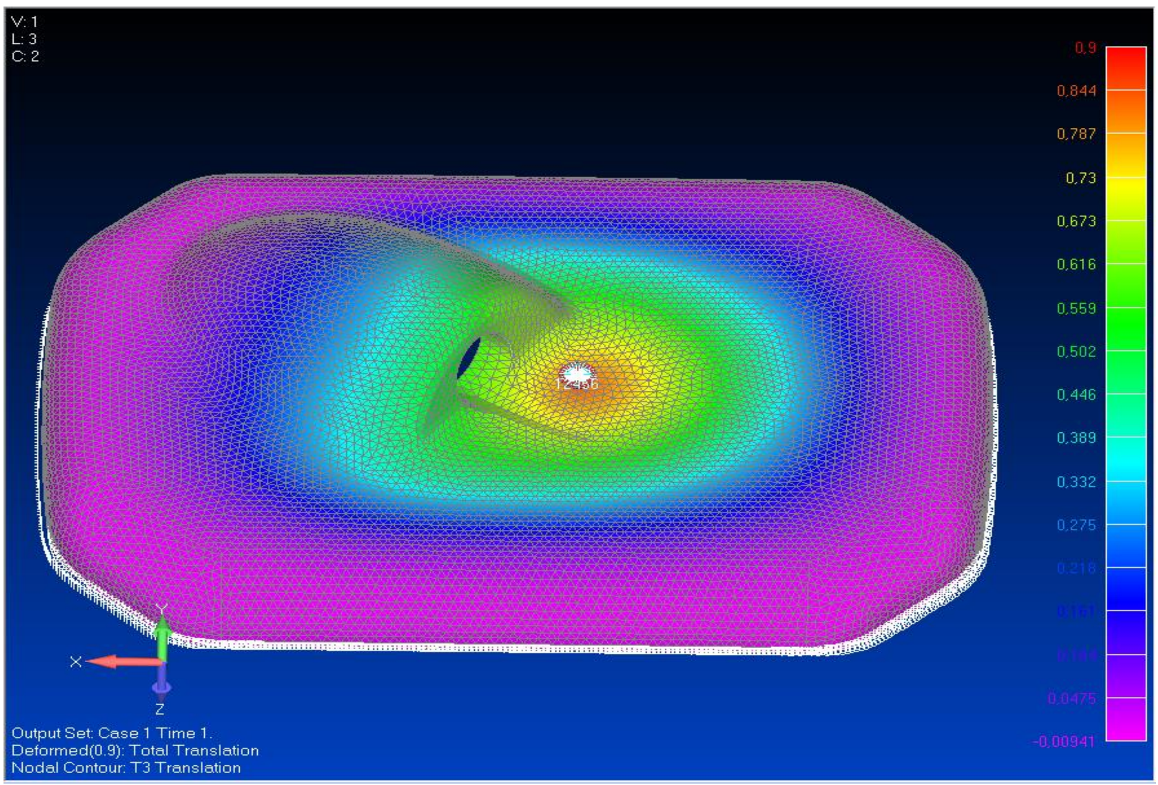

Fig 17: Bottom part

The input values for this analysis are given as mentioned earlier for the Ultem HU 1004. For meshing, second degree elements are used. Since it is a non-linear elastic model, stress-strain curves are used to define the non-linearity. A force of 100 N is applied through the impactor (resembling the teeth), and the corresponding deflection is observed. Fully clamped constrain conditions are implemented for the simulation and advance non-linear solver is used for the analysis.

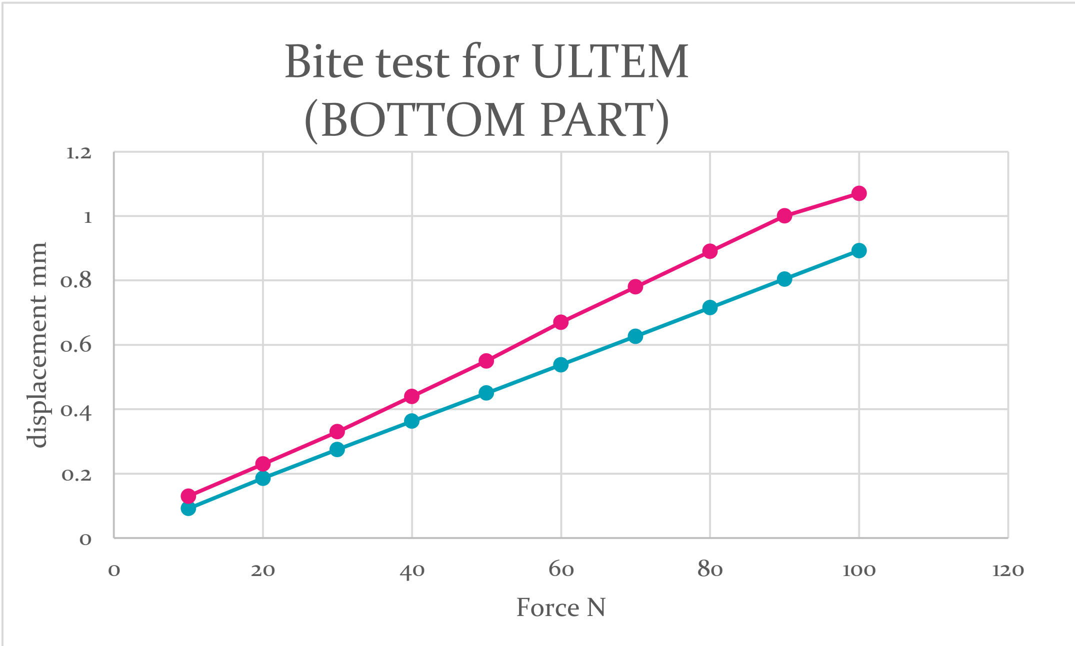

Fig 18: Results from the simulation and real test data

Once the analysis is complete, the load-deflection curve is generated as can be seen in fig 18. The pink line represent graph from the real test while the blue line represent the graph from the simulation. The deflection achieved through the simulation is 0.89 mm while in real life the deflection is 1.07mm. There is 16.5 % less deflection achieved in the simulation. It appears to be that the model is stiffer than the actual structure.

When the effect on the result is observed by changing different input parameters, it appears to be that changing the young's modulus in a non-linear elastic model has no effect on the result. However, change in Poisson's ratio has some effect on the result (Table 2).

Poisson ratio	Deflection(mm)
0.3	0.91
0.36	0.89
0.45	0.83

Table 2: Effect of Poisson's ratio on simulation result

To see the effect of different constrain condition, several constrains are changed. By allowing translation in x-direction, the results gets a bit closer to the desired value. However, allowing translation in y direction or x-y combined, the result goes far more offset than the real test data. The results for the simulations are in fig 19.

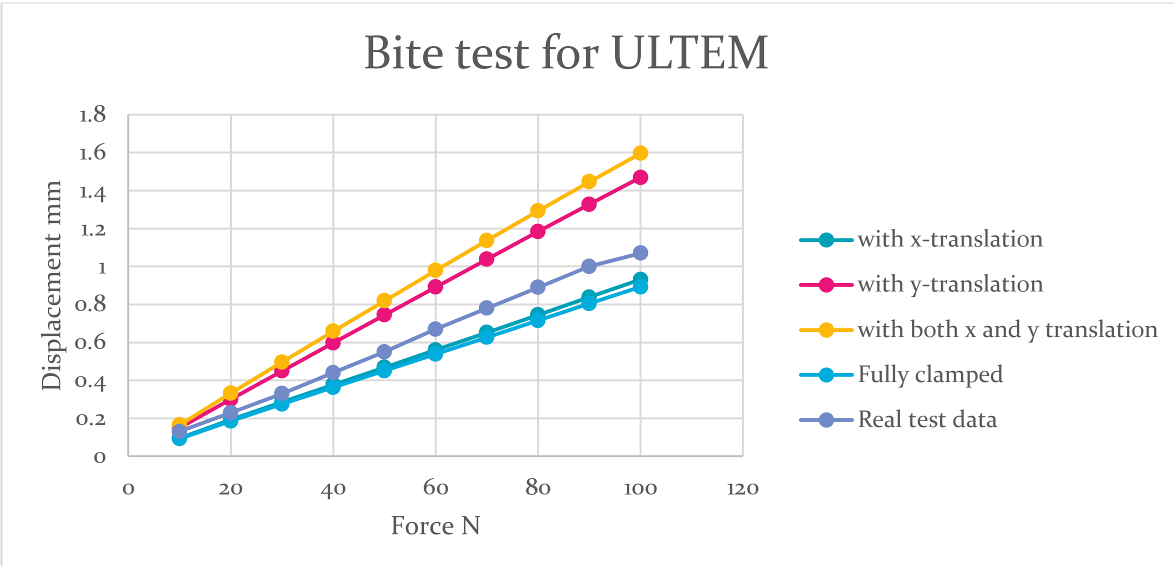

Fig 19: Simulation with varying constrains for the bottom part.

Top part

In fig 20, the top half of the structure can be seen:

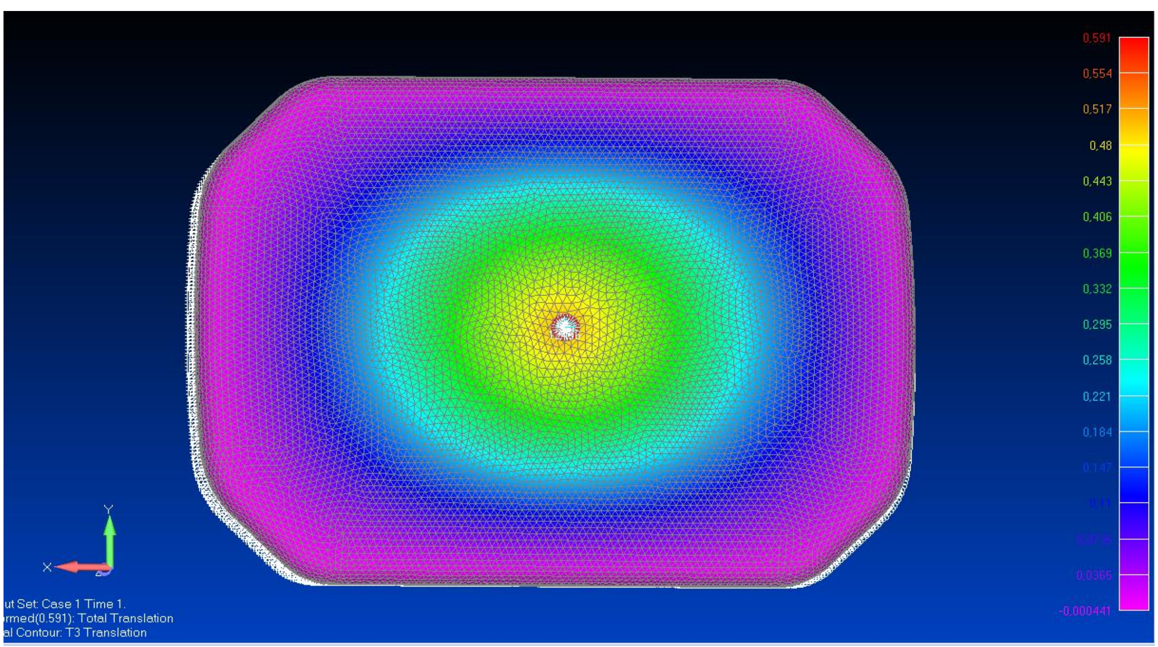

Fig 20: Top Part

Same input parameters, constrains, load and solvers are used for the top part as it was for the bottom part. After the simulation is complete, load-displacement graph is generated and is given in fig 21:

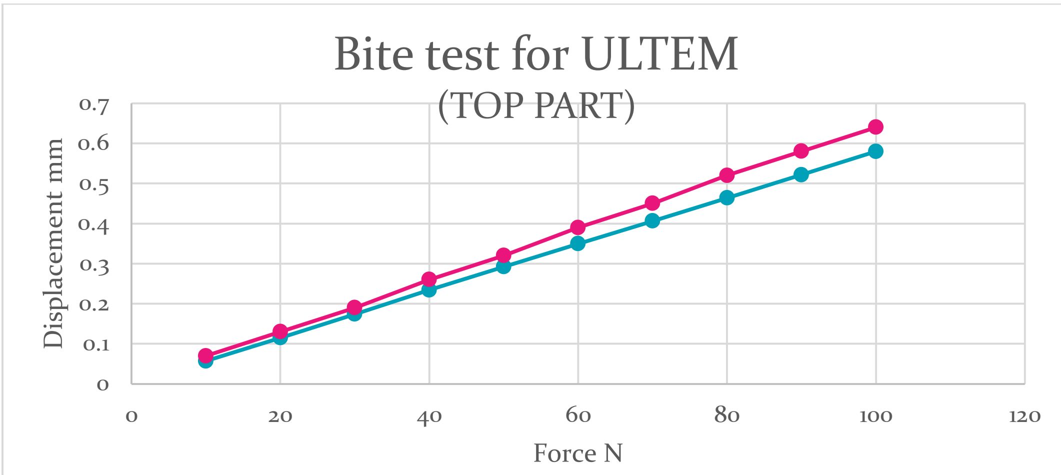

Fig 21: Results from simulation and real test data

The pink line represent graph from the real test while the blue line represent the graph from the simulation. The deflection achieved through the simulation is 0.58 mm while in real life the deflection is 0.64mm. There is 9 % less deflection achieved in the simulation. It also appears to be that the model is stiffer than the actual structure as like it was for the bottom part.

Several simulations are run with varying constrains for the top cover too with the same motive to see whether results close to real test data can be achieved. The results for the simulations are in fig 22.

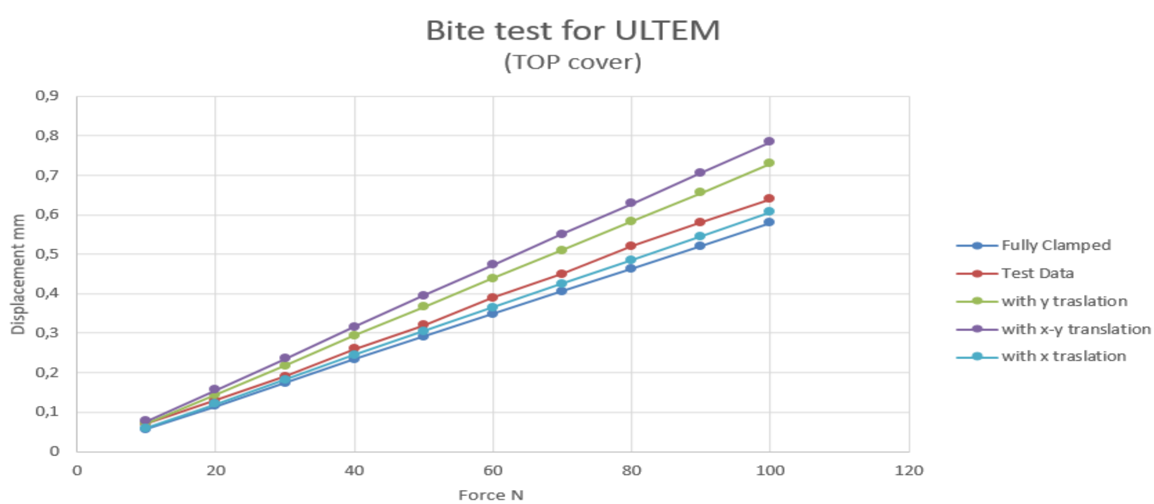

Fig 22: Simulations with varying constrains for the top part

Similarly the result converges slightly towards the desired value when translation in the x-direction is allowed. But allowing translation in the y-direction or x-y combined, the result goes further away from the real test data.

It can be concluded that, constrains are not the reason for not achieving the exact result in the simulation.

In addition to non-linear elastic model, a plastic model is also developed for both bottom and top part to check whether it gives better results. Data in table 3 are used for developing the plastic model.

Yield stress

Stress (MPa)	strain
0	0
54	0.0186
75	0.03
87	0.04
95	0.05
97	0.055
99	0.06
101	0.07

E= 2900 MPa

Table 3: Input data for plastic model

Comparison				
	Bottom part		Top Part	
	mm		mm	
Real test data	**1.07**		**0.64**	
	Considering Engineering stress-strain	Considering True stress-strain	Considering Engineering stress-strain	Considering True stress-strain
Old simulation	0.69	0.67	0.54	0.53
Current simulation (with geometric non linearity)	0.89	0.87	0.58	0.56
Current simulation (without geometric non-linearity)	0.86		0.54	
Current simulation (with plastic model)	0.86		0.57	
Percentage improved in result compared to old result	22.5%		6.9%	

Table 4: comparison of various simulation

As discussed earlier and also can be seen from table 4 that the simulation results for both bottom and top part vary with certain offset from the real test result. It can be due to the fact that the material property is not constant throughout the material due to manufacturing error. But a certain improve in the current simulation results can be observed from the table compare to old simulations (that was carried out using different FE software). This can be due to the usage of different software that uses different solver when running the simulation. Also, considering geometric non-linearity plays a part in giving better result which was not considered in old simulation.

The plastic model however didn't produce better result than the existing non –linear elastic model as can be seen in table 4.

7. CONCLUSION

After a brainstorming 11 weeks, the FE model for tensile and flexure test specimen for plastic material is made, validated, and implemented on an existing FE model. It all started with literature study where various information is found and put together to build an efficient model. Based upon these information, two tensile test FE model and one flexure test FE model are developed maintaining the international standards.

For the FE model of the tensile test specimen with bilinear properties, it can be concluded that the FE model works fine except for a particular region, where it overestimates the strength of the material. The elongation between nodes as the applied forced displacement increases can also be followed within the FE model.

As far as flexure test FE model is concerned, it is able to take non-linearity (the case for plastic material) into consideration, and give the value of the flexure modulus different than that of tensile.

For the validation, real test data are fed into the FE model and the behavior is observed. When the results are compared, it matches with the experimental results suggesting that the FE model works well.

Finally several simulation are run on a plastic structure to see the deflection from a bite test. When compared with the experimental data, the simulation results differ up to 16%. It can be that the material properties are not maintained equally all through the structure due to manufacturing error.

8. WORKING ENVIRONMENT

I would describe the ideal working environment as one that makes the most of my qualifications and abilities, and gives me a chance to constantly challenge myself. My internship consists of quality supervision, a positive work culture that encouraged me to work at my best.

I was given a solid working guideline from the very beginning that helped me to be in track and meet deadlines in order to finish my internship on time. I was provided with my own working table with two big monitors with necessary working tools installed in it. My colleagues were very helpful and supportive. They helped me whenever I was stuck and encouraged me to ask as many question as possible in order to get used to the company's way of working. This made me feel more welcomed and comfortable. During lunch break, everyone eats Dutch lunch (provided by the company) in the lunch room. This creates good social interaction and helps to integrate with colleagues in very short time. My supervisor had meeting with me every week to discuss my progress and guide me to the next step.

My workplace gave me enough space and helped me to grow. I experienced healthy team work, good communication, mutual understanding between each of my colleagues. A workplace where there is respect for individual's ideas and always appreciate good work as well as knowledge.

Bibliography

[1] ASTM. [Online]. Available: https://wenku.baidu.com/view/8ed035116c175f0e7cd13758.html?re=view. [Accessed 29 08 2017].

[2] Sabic. [Online]. Available: https://www.sabic-ip.com/gepapp/eng/weather/weatherhtml?sltUnit=SI&sltRegionList=1002002000&sltPrd=1002003008&sltGrd=1002019084&sltModule=DATASHEETS&sltType=Online&sltVersion=Internet&sltLDAP=0. [Accessed 29 8 2017].

[3] ISO. [Online]. Available: https://wenku.baidu.com/view/05d1334cf524ccbff02184b6.html?from=search. [Accessed 29 08 2017].

[4] ASTM. [Online]. Available: https://wenku.baidu.com/view/10e33f8583d049649b6658f6.html?from=search. [Accessed 29 08 2017].